Micromechanical resonators fabricated from lattice-matched and etch-selective GaAs/InGaP/GaAs heterostructures

Seung Bo Shim, June Sang Chun,[a] Seok Won Kang,[b] Sung Wan Cho, Sung Woon Cho, and Yun Daniel Park[c]
FPRD Department of Physics and Astronomy, Seoul National University, Seoul 151-747, Korea

Pritiraj Mohanty
Department of Physics, Boston University, 590 Commonwealth Avenue, Boston, Massachusetts 02215, USA

Nam Kim and Jinhee Kim
Leading Edge Technology Group, Korea Research Institute of Standards and Science, Daejeon 306-600, Korea

(Received 27 July 2007; accepted 7 September 2007; published online 26 September 2007)

Utilizing lattice-matched GaAs/InGaP/GaAs heterostructures, clean micromechanical resonators are fabricated and characterized. The nearly perfect selectivity of GaAs/InGaP is demonstrated by realizing paddle-shaped resonators, which require significant lateral etching of the sacrificial layer. Doubly clamped beam resonators are also created, with a Q factor as high as 17 000 at 45 mK. Both linear and nonlinear behaviors are observed in GaAs micromechanical resonators. Furthermore, a direct relationship between Q factor and resonant frequency is found by controlling the electrostatic force on the paddle-shaped resonators. For beam resonators, the dissipation (Q^{-1}) as a function of temperature obeys a power law similar to silicon resonators. © *2007 American Institute of Physics*.

[DOI: 10.1063/1.2790482]

In addition to the many technological applications of micro- and nanoelectromechanical systems (MEMS/NEMS), these structures have proven invaluable in fundamental research. This practicality is especially true in experiments where very small interacting forces are studied.[1] Most of the NEMS resonating structures currently used are based on single-crystal Si fabricated from silicon-on-insulator substrates, as the mechanical and electrical properties of these systems are well-known and processing techniques are well developed. Recently, there have been efforts to utilize other materials with particularly high Young's modulus, such as aluminum nitride,[2] silicon carbide,[3] and ultrananocrystalline diamond.[4] Yet, GaAs-based NEMS represent an important alternative; although they have modest mechanical properties, resonators based on this material are more easily integrated with high-speed electronics and intrinsic piezoelectric properties can be utilized as displacement sensing mechanisms.[5] From the optical cooling of mechanical micromirrors[6] to the mechanical manipulation of spin,[7] GaAs-based resonators can be integrated with a wide range of optical, mechanical, and electronic elements. Thus, a reliable way of crafting clean GaAs NEMS resonators would be of great benefit to fundamental research.

The sensitivity of a NEMS resonator to ultrasmall forces is governed by continuum mechanics, at least to first order. As an illustration of this principle, in mass sensing applications the flexural resonant frequency of a doubly clamped beam resonator can be expressed as $f_0=(1.03)\sqrt{E/\rho}(t/l^2)$, where t is the thickness of the beam and l is its length. Thus, increasing the mass of the resonator will change its resonant frequency. The degree to which this change can be accurately measured also depends on the Q factor of the resonator. The Q factor (or Q^{-1} dissipation) of a NEMS structure is determined by many different factors; however, empirical observations indicate that it decreases along with the resonator's dimensions.[8] At low temperatures, however, even Si NEMS resonators are dominated by surface effects: their dissipation characteristics are more suggestive of glassy systems than single crystals.[9] The relationship between the internal stress of flexural beams and the Q factor has recently been found to play a critical role in high-stress silicon nitride resonators and single crystal Si NEMS resonators.[10]

The purpose of this letter is to characterize a new variety of GaAs NEMS resonator. Our structures are realized from lattice-matched GaAs/InGaP/GaAs heterostructures, and fabricated without any plasma processing. GaAs is also an interesting material choice for MEMS applications, as its piezoelectric properties interface well with optoelectronic components. Furthermore, the micromachining techniques used for GaAs and related heterostructures are now well developed in large part owed to advances in optoelectronic device applications.[11]

Most GaAs microresonators reported in the literature are fabricated from GaAs/AlGaAs heterostructures, which require a trade-off between etch selectivity and lattice match with the Al content. The technique described here demonstrates the suitability of InGaP as a sacrificial layer by realizing and releasing a paddle-shaped GaAs resonator, which requires a significant amount of lateral etching. We demonstrate a nearly perfect etching chemistry for lattice-matched GaAs/InGaP heterostructures,[12] achieving both paddle-shaped and doubly clamped beam resonators without the need for plasma processing.

Our micromechanical resonators are realized from lattice-matched undoped GaAs(500 nm)/$In_{0.49}Ga_{0.51}P$(500

[a]Present address: Hynix Semiconductor, Icheon, Korea.
[b]Present address: Samsung LCD, Cheonan, Korea.
[c]Electronic mail: parkyd@phya.snu.ac.kr

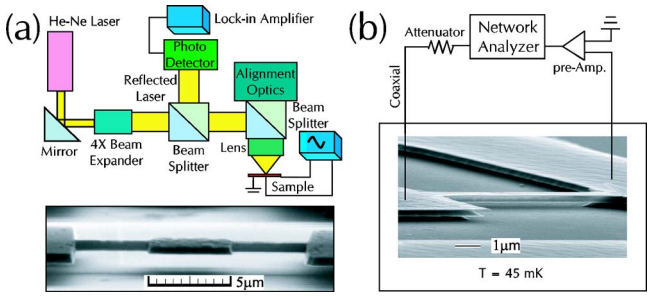

FIG. 1. (Color online) Schematic of the experiment, with SEM images of the resonators. The optical measurement is depicted in (a); note that the paddle-shaped resonator is electrostatically driven. A rf lock-in amplifier reads the photodetector signal. All optical measurements are carried out at room temperature. For doubly clamped resonators, a schematic of the magnetomotive technique is shown in (b).

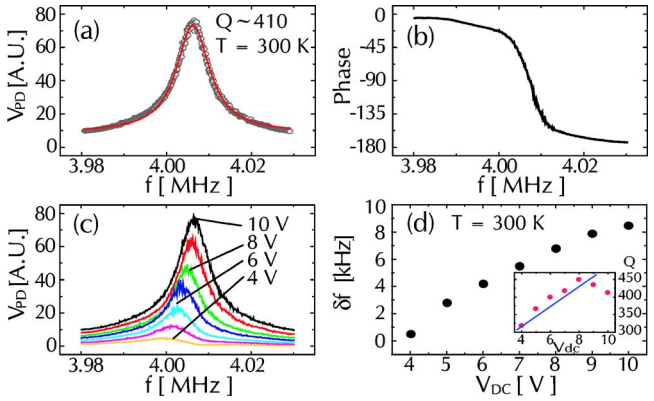

FIG. 2. (Color online) The amplitude (a) and phase (b) of a GaAs paddle-shaped resonator as a function of driving frequency. The solid line in (a) traces a Lorentzian fit. The resonant frequency is 4.006 MHz, with a quality factor of 410. Changes in the resonant frequency as a function of applied bias are plotted in (c) and (d). Changes in the *Q* factor are plotted in the inset of (d).

nm)/semi-insulating GaAs(001) substrates.[13] Epifilms are grown by Epiworks, Inc. (Champaign, IL) using metal-organic chemical vapor deposition. Resonators are patterned along the [100] direction by a combination of standard e-beam and photolithography techniques. This is followed by lift-off of the physical vapor-deposited metallic layers, typically Ti(5 nm)/Au(50 nm), which also serve as an etch mask. The GaAs layer is defined by a standard citric acid/hydrogen peroxide solution, and the process is carefully monitored to minimize lateral etching below the metallic mask. The resonator structures are then released by removing the InGaP sacrificial layer with an HCl solution. The paddle-shaped resonators are characterized at room temperature and an ambient pressure of ~80 kPa. The beam resonators are characterized in a commercially available ^{3}He cryostat with a 9 T superconducting magnet or a dilution refrigerator cryostat with an 8 T magnet. These experiments are depicted in Fig. 1, along with images of the resonators themselves.

Optical interferometry is used to detect the displacement of the paddle-shaped resonators [Fig. 1(a)].[14] A HeNe laser (λ=633 nm) with a beam diameter less than 2 μm is focused on the paddle-shaped resonator using a long-distance objective lens. The paddle-shaped resonators are actuated electrostatically with a sinusoidal waveform. Reflected light is detected by a high-bandwidth photodetector whose signal is fed into a rf lock-in amplifier.

The paddle-shaped resonator's fundamental response to various electrostatic signal frequencies is plotted in Figs. 2(a) and 2(b). For these data, the resonator has a 5 μm×5 μm×500 nm paddle and two 1 μm×5 μm ×500 nm support beams. Near ambient conditions, the resonant frequency is 4.0065 MHz with a *Q* factor of ~410. We attribute this frequency to the fundamental translation mode. We can increase the tension in the resonator by adjusting the dc bias, which determines the electrostatic force between resonator and substrate. This leads to an increase in the resonant frequency [Figs. 2(c) and 2(d)]. As reported by Verbridge *et al.*,[10] we also note that *Q* increases with tension [Fig. 2(d) inset].

Doubly clamped beam resonators are characterized by the standard magnetomotive technique [Fig. 1(b)].[1] The resonator has dimensions of 0.5 μm×0.5 μm×15 μm and is placed inside a ^{3}He refrigerator (260 mK base temperature) in high vacuum (10^{-6} Torr). The long axis of the resonator is perpendicular to a magnetic field generated by 9 T superconducting magnet. A network analyzer generates an alternating current along the length of the resonator. The current moves the beam by generating an oscillating Lorentz force. The beam's motion in the magnetic field induces an emf, which is read by the network analyzer.

The fundamental response of a doubly clamped beam is plotted in Fig. 3(a). The resonant frequency is 17.978 MHz, and the quality factor is ~11 000—nearly an order of magnitude higher than that of similar GaAs resonators realized from GaAs/AlGaAs heterostructures.[5] Figure 3(b) shows the onset of nonlinear behavior as the driving current increases (inset), as well as the corresponding V_{emf} resonances. Such nonlinear effects in NEMS structures may find practical applications in ultrasmall force sensors,[15] memory elements,[16] and signal processors.[17] Figure 3(c) shows the expected quadratic dependence between the displacement signal and the

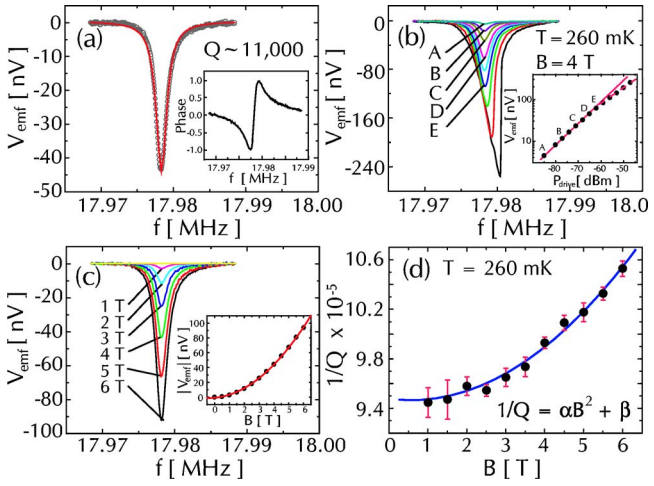

FIG. 3. (Color online) A GaAs doubly clamped beam resonator is characterized by the magnetomotive technique. The resonant frequency is 17.978 MHz, with a *Q* factor of 11 000 (a). A Lorentzian fit to the data is shown as a solid line. The inset shows the corresponding phase information. The responses of the system to different driving amplitudes at a fixed temperature (260 mK) and magnetic field (4 T) are plotted in (b). The induced EMF increases linearly with driving amplitude up to −60 dBm. The points A, B, C, D, and E represent −85, −77, −71, −65, and −62 dBm, respectively. The effect of magnetic field intensity on the resonance is depicted in (c); the inset depicts the expected quadratic behavior. Finally, (d) demonstrates the quadratic dependence of dissipation on the applied magnetic field. The error bars are derived by fitting a Lorentzian function to the resonances.

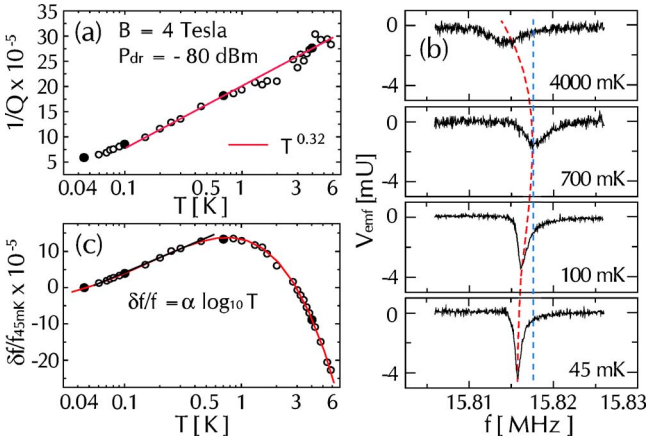

FIG. 4. (Color online) For these data, a GaAs doubly clamped beam resonator similar to that characterized in Fig. 3 is placed in a dilution refrigerator with an 8 T superconducting magnet and a base temperature of 45 mK. The resonator is actuated with −80 dBm in a 4 T field. The temperature dependence of the energy dissipation Q^{-1} is shown in (a). The energy dissipation increases according to the power law $Q^{-1} \sim T^{0.32}$. Degradation of the mechanical resonance is evident in (b), which shows the frequency shift as a function of temperature. The dashed lines are drawn as a guide to the eye. The Q factor decreases from 17 000 to 3500 as the temperature increases from 45 mK to 4 K. The temperature dependence of the resonant frequency is shown in (c); logarithmic behavior appears below ~0.7 K.

applied magnetic field. Figure 3(d) demonstrates the expected monotonic increase in dissipation with magnetic field intensity (or actuation amplitude). The quadratic appearance of Fig. 3(d) suggests the presence of charged defects or impurities.

To better understand the dissipation mechanism in these resonators, we measure the dissipation (Q^{-1}) and resonant frequency shift ($\delta f/f$) of a doubly clamped beam resonator between room temperature and 45 mK. The dimensions and properties of this resonator are similar to those just described (Fig. 3). Both terms approximate the susceptibility function $\chi(\omega_0) \propto (2\delta f/f + iQ^{-1})$, which describes the mechanical response of a system to its environment near resonance. Figure 4(a) shows that the dissipation has a weak power law dependence on temperature $Q^{-1} \sim T^{0.32}$. This dependence is similar to the behavior of single-crystal Si resonators, where the dissipation increases as $T^{0.36}$. These observations agree with a recent theoretical calculation[18] of low-temperature dissipation in tunneling two-level systems, where $Q^{-1} \propto T^{1/3}$ is expected. The resonance shift [Figs. 4(b) and 4(c)] increases with temperature up to ~0.7 K, then decreases. The slightly asymmetric shape of the responses near resonance at low temperatures [Fig. 4(b)] may be related to a small intrinsic nonlinearity of the structure.[9]

In conclusion, we have realized paddle- and beam-shaped GaAs microresonators from GaAs/InGaP/GaAs heterostructures. This achievement demonstrates the suitability of InGaP as a sacrificial layer. Furthermore, we have achieved resonators with exceptionally high Q factors by avoiding plasma processing techniques. The resonators behave similarly to previously reported NEMS structures, demonstrating a similar increase in resonant frequency and Q factor by controlling tension, nonlinear dynamics, and temperature dependence of dissipation.

This work is supported by the Korea Research Foundation Grant, funded by the Korean Government (MOEHRD, Basic Research Promotion Fund) (KRF-2006-311-C00297). It is partly supported by KOSEF, through CSCMR and MOCIE. Y.D.P. is partly supported by City of Seoul R&BD.

[1] A. N. Cleland, *Foundations of Nanomechanics* (Springer, Berlin, 2002).
[2] A. N. Cleland, M. Pophristic, and I. Ferguson, Appl. Phys. Lett. **79**, 2070 (2001).
[3] Y. T. Yang, K. L. Ekinci, X. M. H. Huang, L. M. Schiavone, M. L. Roukes, C. A. Zorman, and M. Mehregany, Appl. Phys. Lett. **78**, 162 (2001).
[4] M. Imboden, P. Mohanty, A. Gaidarzhy, J. Rankin, and B. W. Sheldon, Appl. Phys. Lett. **90**, 173502 (2007).
[5] A. N. Cleland, J. S. Aldridge, D. C. Driscoll, and A. C. Gossard, Appl. Phys. Lett. **81**, 1699 (2002); R. Knobel and A. N. Cleland, *ibid.* **81**, 2258 (2002); H. X. Tang, X. M. H. Huang, M. L. Roukes, M. Bichler, and W. Wegscheider, *ibid.* **81**, 3879 (2002); R. G. Knobel and A. N. Cleland, Nature (London) **424**, 291 (2003).
[6] S. Gigan, H. R. Bohm, M. Paternostro, F. Blaser, G. Langer, J. B. Hertzberg, K. C. Schwab, D. Bauerle, M. Aspelmeyer, and A. Zeilinger, Nature (London) **444**, 67 (2006); D. Kleckner and D. Bouwmeester, *ibid.* **444**, 75 (2006).
[7] J. A. H. Stotz, R. Hey, P. V. Santos, and K. H. Ploog, Nat. Mater. **4**, 585 (2005); H. Knotz, A. W. Holleitner, J. Stephens, R. C. Myers, and D. D. Awschalom, Appl. Phys. Lett. **88**, 241918 (2006).
[8] P. Mohanty, D. A. Harrington, K. L. Ekinci, Y. T. Yang, M. J. Murphy, and M. L. Roukes, Phys. Rev. B **66**, 085416 (2002).
[9] G. Zolfagharkhani, A. Gaidarzhy, S. B. Shim, R. L. Badzey, and P. Mohanty, Phys. Rev. B **72**, 224101 (2005).
[10] S. S. Verbridge, J. M. Parpia, R. B. Reichenbach, L. M. Bellan, and H. G. Craighead, J. Appl. Phys. **99**, 124304 (2006); S. S. Verbridge, D. F. Shapiro, H. G. Craighead, and J. M. Parpia, Nano Lett. **7**, 1728 (2007).
[11] K. Hjort, J. Micromech. Microeng. **6**, 370 (1996).
[12] J. Lothian, J. Kuo, F. Ren, and S. Pearton, J. Electron. Mater. **21**, 441 (1992); M. J. Cich, J. A. Johnson, G. M. Peake, and O. B. Spahn, Appl. Phys. Lett. **82**, 651 (2003).
[13] H. K. Choi, J. S. Lee, S. W. Cho, W. O. Lee, S. B. Shim, and Y. D. Park, J. Appl. Phys. **101**, 063906 (2007).
[14] S. Evoy, D. W. Carr, L. Sekaric, A. Olkhovets, J. M. Parpia, and H. G. Craighead, J. Appl. Phys. **86**, 6072 (1999).
[15] M. V. Requa and K. L. Turner, Appl. Phys. Lett. **90**, 173508 (2007).
[16] R. L. Badzey, G. Zolfagharkhani, A. Gaidarzhy, and P. Mohanty, Appl. Phys. Lett. **85**, 3587 (2004).
[17] R. L. Badzey and P. Mohanty, Nature (London) **437**, 995 (2005); R. Almog, S. Zaitsev, O. Shtempluck, and E. Buks, Appl. Phys. Lett. **90**, 013508 (2007); S. B. Shim, M. Imboden, and P. Mohanty, Science **316**, 95 (2007).
[18] C. Seoanez, F. Guinea, and A. H. Castro Neto, Europhys. Lett. **78**, 60002 (2007).